NANOSYSTEMS: PHYSICS, CHEMISTRY, MATHEMATICS, 2019, 10 (4), P. 410–414

Quantum image transmission based on linear elements

P. A. Gilev, I. Y. Popov

ITMO University, Kronverkskiy, 49, St. Petersburg, 197101, Russia

grandarchtemplar@gmail.com, popov1955@gmail.com

PACS 03.67.Hk, 42.50.Ex **DOI 10.17586/2220-8054-2019-10-4-410-414**

Modeling of image transmission with a classic quantum computer interpreter is suggested. The transmission algorithm from the paper (Lemos G.B., et.al. Quantum Imaging with Undetected Photons, *Nature*, 2014, **512**, P. 409–412) is modified to reduce the complexity of the quantum circuit. Simplification was done by replacing the non-linear optical elements with a conventional quantum entanglement operator. The obtained results show expected efficiency of data transmission with Gaussian beam by hypothesis test and calculation error function. This error function is used for quality measurement. The interpreter is written in Kotlin language.

Keywords: quantum imaging, quantum communication, image restoration.

Received: 7 June 2019

Revised: 3 August 2019

1. Introduction

The production of a working quantum computer has become a real possibility thanks to recent developments in the field of nanotechnology but there is still a long way to go [1]. Optical channels are preferable in quantum communications (see, e.g., [2, 3]). The idea of quantum signal transportation appeared at the very beginning of quantum algorithms research or even earlier. The AbbeRayleigh diffraction limit constrains spatial resolution for classical imaging methods. Quantum imaging exploits correlations between photons to reproduce structures with higher resolution. Quantum-correlated N-photon states were shown to potentially surpass the classical limit by a factor of $1/N$, corresponding to the Heisenberg limit, using a method known as optical centroid measurement [4–6]. Quantum imaging found many applications in communications, material investigation, biology, etc. [7–10].

The measurement problem discovered by Steven Weinberg in 1998 [11] does not give one the ability to use full information contained in a quantum-entangled system. Thus, measurement avoidance is the main vector of quantum algorithm development, including quantum information transfer algorithm. This leads to the use of an uncontrollably big system in transport system. Other problem is overwhelming difficulty of maintaining an exclusive measurement system. In this way, the measurement of high frequency waves is more difficult than the measurement of low frequency waves. In [12], an example is given of a quantum circuit which transmits information using a wave twice as high frequency as the measured. But this scheme has a problem, elements used in the suggested circuit are difficult for expected behavior simulation. In the present work, we suggest to change all non-linear components by a linear quantum entanglement operator.

2. Quantum imaging

2.1. Classic quantum computer interpreter

A modified quantum imaging algorithm is implemented with classic quantum computer interpreter. The main element of the quantum algorithm is *unitary* operators. Operator A is called unitary operator if $AA^+ = A^+A = E$ where E is the identity operator and A^+ is the adjoint operator. Each unitary operator corresponds to some quantum operation (quantum gate) applied to quantum system. A composition of two unitary operators is consequent application of each one. A sequence of quantum gates forms a quantum algorithm.

Qubit is the main object for quantum computing. A physical qubit is a quantum system which can be in a superposition of two states. In quantum informatics, any system has 2^n states where n is the number of qubits. Each qubit is a complex 2-vector

$$|\phi\rangle = \begin{pmatrix} \alpha \\ \beta \end{pmatrix}, \quad \alpha, \beta \in \mathbb{C},$$

where $|\alpha|^2, |\beta|^2$ are the probabilities of observing the qubit in the corresponding state, respectively, $|\alpha|^2 + |\beta|^2 = 1$.

The state space for a multiqubit system is the tensor product of the state spaces for separate qubits. Let A be the operator acting on the first qubit $|\phi\rangle$ and B be the operator acting on the second qubit $|\psi\rangle$. Then,

$$(A \otimes B)(|\phi\rangle \otimes |\psi\rangle) = A(|\phi\rangle) \otimes B(|\psi\rangle),$$

where $\otimes$ is the tensor product of operators (in matrix case, it is the Kronecker product of matrices). Particularly, the tensor product of two vectors $|\phi\rangle, |\psi\rangle$ of sizes $n \times 1, m \times 1$ is the vector ξ of size $nm \times 1$, where:

$$\xi_{ni+j} = \phi_i \psi_j \ \forall i \in (1 \dots n), \forall j \in (1 \dots m).$$

The tensor product of two matrices A, B of sizes $n \times n, m \times m$ is the block matrix C with the following block entries

$$C_{ij} = A_{ij} B \ \forall i, j \in (1 \dots n).$$

So for implementation of a classic quantum interpreter, the following operations should be implemented:

(1) Algebra of application of matrix to vectors,
(2) Algebra of multiplication between two matrices,
(3) Algebra of tensor products between two vectors,
(4) Algebra of tensor products between two matrices.

2.2. Implementation features

In the current work some data structures were recreated to fulfill the requirements of clean functional style code. Thus, the vector is linked list with generalized typing. Also the full experimental model used complex number type which does not exist in vanilla Kotlin. The main idea is to use only recursive types with single exit point for tail-optimization provided by JVM environment. These types of structures also solve the problem of state mutation, as, all elements are made immutable objects.

Because the Kotlin sealed class model does not allow to extend them beyond this class, there are some features such as boxed types. Any type used for this interpreter are boxed. So, formally, there are no outer usage of standard types.

Finally, there is a problem that Kotlin does not have an apparatus for contract checking, as for pure functions so for impure. Also, it can not guarantee that all objects are linear-typing. So, the usage of this interpreter is non-verified and thus, there is a need for large test coverage or in formal verification. For image processing the standard java library is used.

2.3. Gaussian beam model

The main transmitter is a laser with Gaussian beam characteristics. A Gaussian beam is one in which there is a superposition of coherent waves each of which has special distribution of amplitudes:

$$H_{ij}(x, y) = H_i(\frac{x\sqrt{2}}{\rho}) H_j(\frac{y\sqrt{2}}{\rho}) e^{-\frac{x^2+y^2}{\rho}},$$

where ρ is related to the width of the beam, $H_i(x)$ is the Hermitian polynomial

$$H_i(x) = \sum_{j=0}^{\lceil n/2 \rceil} (-1)^j \frac{n!}{j!(n-2j)!} (2x)^{n-2j}.$$

Examples of the amplitude distributions can be found below. In Figs. 2–5 one can see the amplitude distributions for main gaussian beam modes which contribute the most important modes for the image.

Also for improvement of statistics, one uses relative distribution without any mode except $|00\rangle, |01\rangle, |10\rangle, |11\rangle$. In the present work, there are attempts to use different sets of Gaussian beams, but it does not confer an essential effect for the quality of the restored image.

The rotation operator is, usually, described by the following matrix in standard basis:

$$T(\phi) = \begin{pmatrix} \cos(\phi) & -\sin(\phi) \\ \sin(\phi) & \cos(\phi) \end{pmatrix},$$

however, we will use another, more convenient, representation:

$$T(t)(\alpha |0\rangle + \beta |1\rangle) = \xi |0\rangle + \zeta |1\rangle,$$

where

$$\xi = \alpha t - \beta \dot{t}, \zeta = \beta t + \alpha \dot{t}, \dot{t} = \sqrt{1 - t^2}$$

Thus, the object can be transformed from a constant matrix to a functional matrix. Here, t is "the rotation function" which is given by location of our beam. In this way, $t : \mathbb{R} \times \mathbb{R} \to \mathbb{R}$. This leads to the final representation of the rotation operator as the following matrix:

$$T(x,y) = \begin{pmatrix} t(x,y) & -\dot{t}(x,y) \\ \dot{t}(x,y) & t(x,y) \end{pmatrix}$$

This rotation operator is a one-qubit operator, but for many-qubit systems, one can consider the corresponding tensor product:

$$T_{k+1} = T \otimes T_k, \quad T_1 = T.$$

Also, one can construct T, not for each pixel (or other atomic element), but for a cluster. This solves a problem of transmission because we can easily facilitate data volume transmitted by classic channel.

Using this operator, one comes to the final representation of the quantum algorithm (the corresponding circuit is shown in Fig. 5):

$$Q = (NL1_{n+n} \otimes E_n) \circ (E_n \otimes T_n(x,y)) \circ (E_n \otimes NL2_{n+n}).$$

Here $NL1$ and $NL2$ elements are non-linear crystals which splits the laser beam in two beams of single frequency. These elements are not simple both for implementation and for computer modelling. We replace it by a linear optical elements (CNOT-gates):

$$Q' = (CNOT_{n+n} \otimes E_n) \circ (E_n \otimes T_n(x,y)) \circ (E_n \otimes CNOT_{n+n})$$

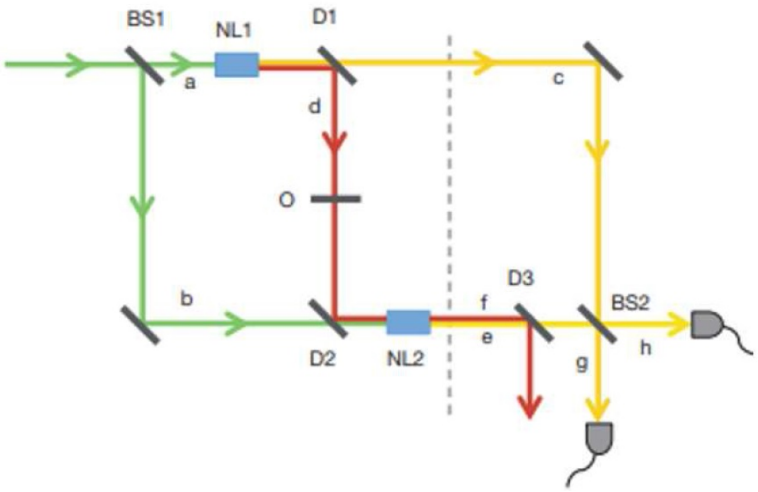

FIG. 1. The main circuit used in [12]

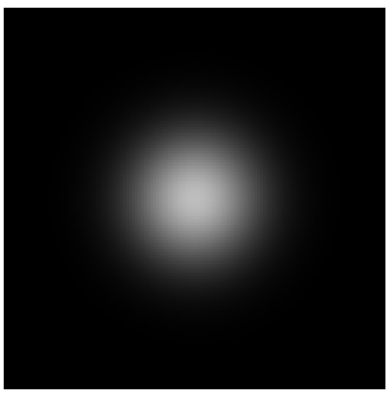

FIG. 2. H_{00} mode distribution

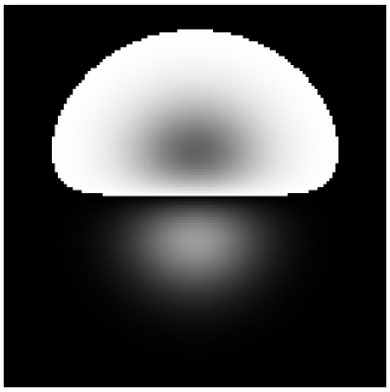

FIG. 3. H_{01} mode distribution

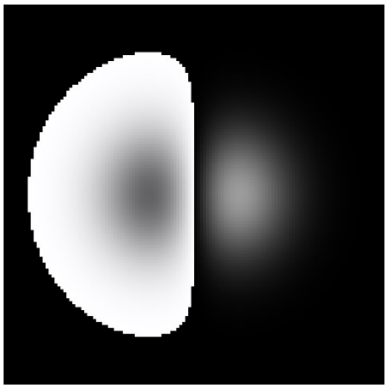

FIG. 4. H_{10} mode distribution

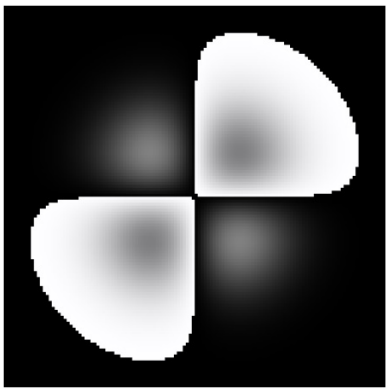

FIG. 5. H_{11} mode distribution

2.4. Measurements with interference model

The measurements are particle numbers which are recorded by the sensors. It is important that the sensors detect only low frequency signals which match them before they have an interference. Taking into account the distribution for the modes, one can calculate the interference between them with simple addition:

$$A(x,y)\dot{+}B(x,y) = I(x,y),$$

where $A(x,y)$ is the distribution after entanglement with modified high-frequency, $B(x,y)$ is the distribution after entanglement with non-modified high-frequency and $\dot{+}$ is the binary operator which sums only projection with right angle. Thus there are two different interference pictures:

$$I_A(x,y) = A(x,y) + T^{+}(x,y)B(x,y),$$

$$I_B(x,y) = T^+(x,y)A(x,y) + B(x,y).$$

Let us perform some pre-transformations. Let $P_h(x,y)$ be the initial high frequency distribution, $P_l(x,y)$ be the initial low frequency distribution, $Z(x,y)$ be the constant zero distribution, $H(x,y)$ be the high frequency after-processed distribution,

$$Q'(P_h \otimes P_l \otimes P_l) = (A \otimes B \otimes H),$$
$$TI_A = TA + TT^+B = TA + B.$$

As A, B are real scalars, their conjugation does not change the inner structure of them.

$$T^+I_A = T^+A + B = I_B,$$

or

$$TI_B = I_A.$$

In this way, we can get A, B if we know nature of T. Keeping in mind the known values of A and B, one can obtain the approximate picture.

Let us estimate the error. MSE (mean squared error) is a metrics for quality of the transmitted image ($I1, I2$ are the initial and the transmitted signals).

$$MSE(I1, I2) = \frac{1}{mn}\sum_{x=1}^{n}\sum_{y=1}^{m}|I1(x,y) - I2(x,y)|^2.$$

The corresponding results for different number of bits is presented in Table 1.

TABLE 1. Results

Size	16	32	64	128	256	512
MSE	0.5601	0.5559	0.5612	0.5603	0.5600	0.5603

3. Conclusion

Finally, the quantum image transmission method was suggested with use of linear elements in quantum circuit (without non-linear ones). This scheme is simpler for implementation than the analogous non-linear ones. It shows an appropriate quality of transmission. But there are two unsolved problems: strong blur on image and the need for classic channel usage (moreover, with no constant size of data). The strong blur may be partially solved by other non-quantum methods or with additional classical data transfer. This need in classic channel, unfortunately, can not currently be resolved by this algorithm without additional complication of the scheme.

Acknowledgements

This work was partially financially supported by the Government of the Russian Federation (grant 08-08), by grant 16-11-10330 of Russian Science Foundation.

References

[1] Milburn G.J., Woolley M.J. Quantum nanoscience. *Contemporary Physics*, 2008, **49**(6), P. 413-433.
[2] Pathak A., Banerjee A. *Optical Quantum Information and Quantum Communication*. SPIE Spotlight, NY, 2016.
[3] Sheremetev V.O., Rudenko A.S., Trifanov A.I. Testing Bell inequalities for multi-partite systems with frequency-encoded photonic qubits. *Nanosystems: Phys. Chem. Math.*, 2018, **9**(4), P. 484–490.
[4] Pittman T.B., Shih Y.H., Strekalov D.V., Sergienko A.V. Optical imaging by means of two-photon quantum entanglement. *Phys. Rev. A.*, 1995, **52**(5), P. R3429–R3432.
[5] Morris P.A., Aspden R.S., Bell J.E.C., Boyd R.W., Padgett M.J. Imaging with a small number of photons. *Nature Commun.*, 2015, **6**, P. 5913/1–6.
[6] Unternahrer M., Bessire B., Gasparini L., Perenzoni M., Stefanov A. Super-resolution quantum imaging at the Heisenberg limit. *Optica*, 2018, **5**(9), P. 1150–1154.
[7] Tenne R. et al. Super-resolution enhancement by quantum image scanning microscopy. *Nat. Photonics*, 2019, **13**, P. 116-122.
[8] Schnell Ch. Quantum imaging in biological samples. *Nature Methods*, 2019, **16**, P. 214–214.
[9] Genovese M. Real applications of quantum imaging. *Journal of Optics*, 2016, **18**, P. 073002.
[10] Kolobov M. (Ed.). *Quantum imaging*. Berlin, Springer, 2007, 111 p.
[11] Weinberg S. The Great Reduction: Physics in the Twentieth Century. In Michael Howard & William Roger Louis (eds.). *The Oxford History of the Twentieth Century*. Oxford University Press, 1998, P. 26
[12] Lemos G.B., Borish V., Cole G.D., Ramelow S., Lapkiewicz R. and Zeilinger A. Quantum Imaging with Undetected Photons. *Nature*, 2014, **512**, P. 409–412.